Original Article

SHM Structural Health Monitoring

Structural Health Monitoring
1–16

DOI: 10.1177/1475921719866439
journals.sagepub.com/home/shm
SAGE

Structural health monitoring of the Ferrara University before and after the 2012 Emilia (Italy) earthquake, and after the damage repairs

Maria Rosaria Gallipoli[1], Tony Alfredo Stabile[1], Giulia Massolino[2], Marco Mucciarelli[2,3], Nasser Abu Zeid[4,5], Leonardo Chiauzzi[3], Samuel Bignardi[4,5,6] and Alessandro Rebez[2]

Abstract

In this article, a framework of building monitoring is developed and transient and permanent variations of the fundamental period of vibration caused by both damage and repair interventions are investigated. The buildings of the University of Ferrara (Emilia-Romagna Region, Northern Italy), struck by the 2012 Emilia seismic sequence, were monitored using both temporary and permanent equipment: the first one to perform ambient vibration tests and the second one to implement permanent real-time monitoring for earthquake recording. Three on-demand ambient vibration tests were performed at each floor of the buildings: the first dataset was acquired a few months before the mainshock occurred on 20 May 2012 (M_L = 5.9, 6.8 km depth and 30 km epicentral distance); the second was acquired right after the end of the sequence, when the building showed slight damage (degree 1 according to the European Macroseismic Scale 98); finally, the third dataset was acquired in 2016 after the repair intervention. The data analysis clearly documented the permanent drop of the first vibration frequency as a symptom of the damage and its partial recovery that followed the repairs. The permanent real-time monitoring system, despite the fact that it was implemented using low-cost sensors, provided an insight into the intra-event frequency variation, allowing in turn a preliminary damage assessment.

Keywords

Structural health monitoring, ambient vibration test, real-time earthquake monitoring, frequency variation, Emilia earthquake

Introduction

Nowadays, structural health monitoring (SHM) represents an important tool for structural safety evaluation and maintenance, damage identification after earthquakes, and aging evaluation. In addition, it represents a cost-effective long-term solution to aid intense planning and operationally demanding repairs and retrofit. In the last two decades, the use of fast monitoring procedures for the structural evaluation of real engineering structures has steadily grown.[1,2] Indeed, SHM plays a major role in the evaluation of the state of health of public/strategic buildings and infrastructure, especially when deciding whether a structure is safe, requires inspection, or must be abandoned. These aspects promoted the current interest in real-time monitoring applications for early warning damage evaluation, which may be conveniently implemented using low-cost sensors.[3,4]

[1]Italian National Research Council (CNR-IMAA), Tito Scalo, Italy
[2]National Institute of Oceanography and Experimental Geophysics (OGS), Sgonico, Italy
[3]School of Engineering, University of Basilicata, Potenza, Italy
[4]University of Ferrara, Ferrara, Italy
[5]School of Electrical and Computer Engineering, Georgia Institute of Technology, Atlanta, GA, USA
[6]CRUST—Interuniversity Center for 3D Seismotectonics with Territorial Applications, Catania, Italy

Corresponding author:
Maria Rosaria Gallipoli, Italian National Research Council (CNR-IMAA), C.da S.Loja, Tito Scalo 85050, Italy.
Email: gallipoli@imaa.cnr.it

SHM is typically implemented by placing sensors in situ in order to monitor the dynamic structural behavior over time. Such time lapse offers several advantages, such as damage detection, definition of its severity and location, and evaluation of structural residual life and vulnerability.

The amplitude and duration of oscillation of a building in response to an earthquake have a profound connection to both the structure's fundamental period and relative damping. As such, they are the most informative parameters when investigating the internal structure of buildings. The most desirable condition to determine their dynamic evolution would be of course by observing seismic events using a permanent monitoring system. However, this solution is typically costly and feasible only in a restricted set of circumstances.[5–9] An alternative to permanent monitoring is using ambient vibration measurements from which the fundamental period and damping can be retrieved using different techniques, namely, horizontal-to-vertical noise spectral ratio (HVNSR),[10–12] standard spectral ratio (SSR),[13] non-parametric damping analysis (NonPaDAn),[14] random decrement method (RDM),[15] and half bandwidth method (HBW),[16] Trifunac[17] and Gallipoli et al.[3,18] confirmed that the fundamental frequency and damping from ambient vibrations are consistent with those obtained by forced vibrations for low input motion and provide a valid reference for a system vibrating within its linear range of behavior. In this study, we estimated the fundamental vibration period and damping of two buildings under low excitation generated by ambient sources such as wind or anthropic activity such as traffic and machinery (in the following, we will generally refer to these signals as "ambient vibration"[11,17,19,20] and weak motions). From these signals, we estimated the lowest natural frequency (f) of vibration of both buildings, henceforth referred to as the first mode of vibration or fundamental period of vibration. In particular, we evaluated this frequency before a specific seismic event and investigated its changes right after the end of the event, after the repair intervention, and, more generally, over time.

The drop of the first vibration frequency, observed during weak and strong motions, might be considered a proxy of the damage.[21,22] As such, over the years, the frequency variation has been widely investigated. The fundamental frequency of buildings is now known to range from 35%, related to the opening of cracks in the elastic domain, up to 60% of permanent drop as the maximum threshold before collapse.[23] After the most recent Italian earthquakes, great effort has been made to quantify the frequency variation corresponding to different levels of damage of reinforced concrete buildings.[24,25] On one hand, we have examples such as the Navelli town hall, which suffered the 2009 Abruzzo earthquake,[26] and the primary school in the Rotonda city struck by the 2010–2014 Pollino swarm.[3] In both cases, the buildings showed multiple temporary period elongations which did not reflect in any increased damage. On the other hand, a permanent period shift accompanied by damage was observed both at a reinforced concrete building located in Bonefro during the 2002 Molise earthquake (Mucciarelli et al., 2004) and at the Mirandola hospital during the 2012 Emilia earthquake.[27] In addition, large datasets of fundamental vibrational frequencies, estimated on reinforced concrete buildings with different levels of damage, were collected by Vidal et al.[24] and Ditommaso et al.[25] after the 2011 Lora and 2009 Abruzzo earthquakes, respectively.

This study is a continuation of the aforementioned research efforts. In particular, we performed two kinds of monitoring on the buildings of the Technological Scientific Pole (PST) of the University of Ferrara (Emilia-Romagna Region, Northern Italy): on-demand ambient vibration tests (AVTs) and real-time earthquake (RTE) monitoring. The AVTs were performed in three different occasions: before the earthquake (April 2012), after the first of the three mainshocks (i.e. the 20 May event and the double-event on 29 May) constituting the seismic sequence (the test dates to 28 May 2012), and 4 years after the repair intervention (September 2016). The peculiarity of this study is that AVTs were performed roughly 1 month before the earthquake that struck the Emilia region on 20 May 2012. The test was not specifically designed for structural investigation purposes and, of course, only part of results from post-earthquake investigations could be compared. Nevertheless, such a fortuitous coincidence provided a convenient opportunity to compare later investigations to an unbiased reference. After the end of the Emilia seismic sequence, two sensors for real-time monitoring were installed: one of them is still in acquisition (Figure 4).

AVTs were useful to evaluate the inter-event variation of the fundamental vibration frequency due to damage,[8,24,25] while the RTE monitoring, by highlighting the intra-event variation, provided real-time damage detection capabilities.[21,28] With such evidence of both temporary and permanent frequency variations, the SHM at this building of the University of Ferrara represents an important case study, showing how changes of the principal structural characteristics, due to both damage and repairs and even during earthquakes, represent a rapid and useful tool for indirect damage detection.

Description of the building monitoring

The May–June 2012 Emilia seismic sequence was characterized by two main events occurred on 20th and 29th

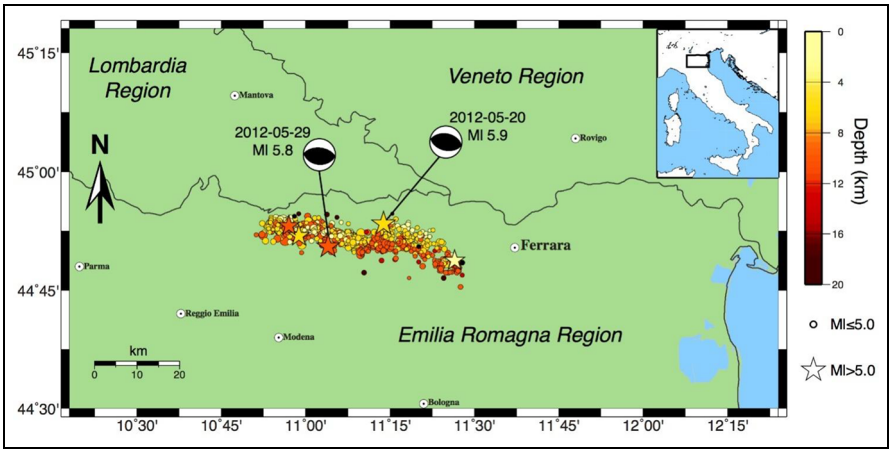

Figure 1. The Emilia seismic sequence of May–June 2012 (seismic data from Govoni et al.).[32] The focal mechanisms of the two mainshocks are displayed. Ferrara and the main cities in the region are highlighted as well.

of May with local magnitudes (M_L) of 5.9 and 5.8, respectively, and several aftershocks including four $M_L > 5$ events[29–32] (Figure 1). The two mainshocks affected numerous towns and cities with Mercalli–Cancani–Sieberg (MCS) intensity values ranging from the V to the VIII degree. The events resulted in 27 casualties and heavy damage to residential, public, and industrial facilities.[27,33] In particular, the MCS intensity at the city of Ferrara reached the V degree[29] mainly due to the strongest shaking on 20 May, when the observed peak ground acceleration (PGA) was of ~0.1g. Indeed, as shown in Figure 1, the epicenters of the sequence migrated westward for about 12 km between the two mainshocks. The epicentral distance from the urban center of Ferrara was 30 and 42 km for the 20 May and 29 May events, respectively.

The investigated structure belongs to the PST of the University of Ferrara (Figure 2(a)). Built in 2002, it features two five-story buildings in reinforced concrete moment resistant frame (Figure 2(c)). The buildings are arranged in L shape (Figure 2(b)) and physically separated by a seismic joint (Figures 3 and 4). They host the Future and Research Consortium ("Consorzio Futuro in Ricerca (CFR)," 50 m × 14.5 m) and the Earth Science Department ("Scienze della Terra (SDT)," 36 m × 14.5 m). The two buildings are similar, but structurally different for number of spans, stair structure location, and dimensions. Concerning plan regularity, stiffness is quite symmetrical with respect to the longitudinal axis, while in the orthogonal direction the stiffness of the resisting elements is strongly asymmetric, mainly because of the presence of the concrete stiff stair structures located in eccentric position. The shallow subsurface constituting the building foundation is mainly composed of clay to silty clay sediments that extend down to 23 m depth, with the presence of thin layers of organic clay followed by a succession of silty sand sediments that reach down to 50 m depth. With an average shear wave velocity in the first 30 m (V_s30) of about 200 m/s, this is according to the Italian Building Code (NTC18), a category "C" site.

On 21 May 2012, the day after the first seismic event, a diagnostic inspection was performed according to the Italian Civil Protection Department procedures.[34,35] The SDT building suffered non-structural damage: few diagonal cracks on the curtain walls of the ground floor and slight damage on the infill walls at the first and second floors. The damage evaluated according to the Italian official procedures assigned slight damage to the infill walls that extended to two-thirds of the structure, and medium to severe damage to the infill walls that extended to one-third of the structure. The global damage state was defined as degree 1 according to the European Macroseismic Scale 1998.[36] In addition, the buildings suffered further non-structural damage such as plaster fall-offs and internal or external object falling. Figure 3 shows the damage assessment at the SDT ground floor along with few related pictures. As a result, the buildings were declared temporarily unsafe—occurrence that caused high discomfort being of public use and workplace to nearly hundred employees. The repair interventions consisted of the following:

Recovery and consolidation of all infill walls at all levels of the building with high-strength mortar and installation of metal mesh;
Recovery and consolidation of the service ducts using 20 modules (five for each floor) which consisted of metallic bars anchored to the corresponding metallic plates (20 cm × 10 cm, thickness 1 cm);
Fixing of all wardrobes and shelves;

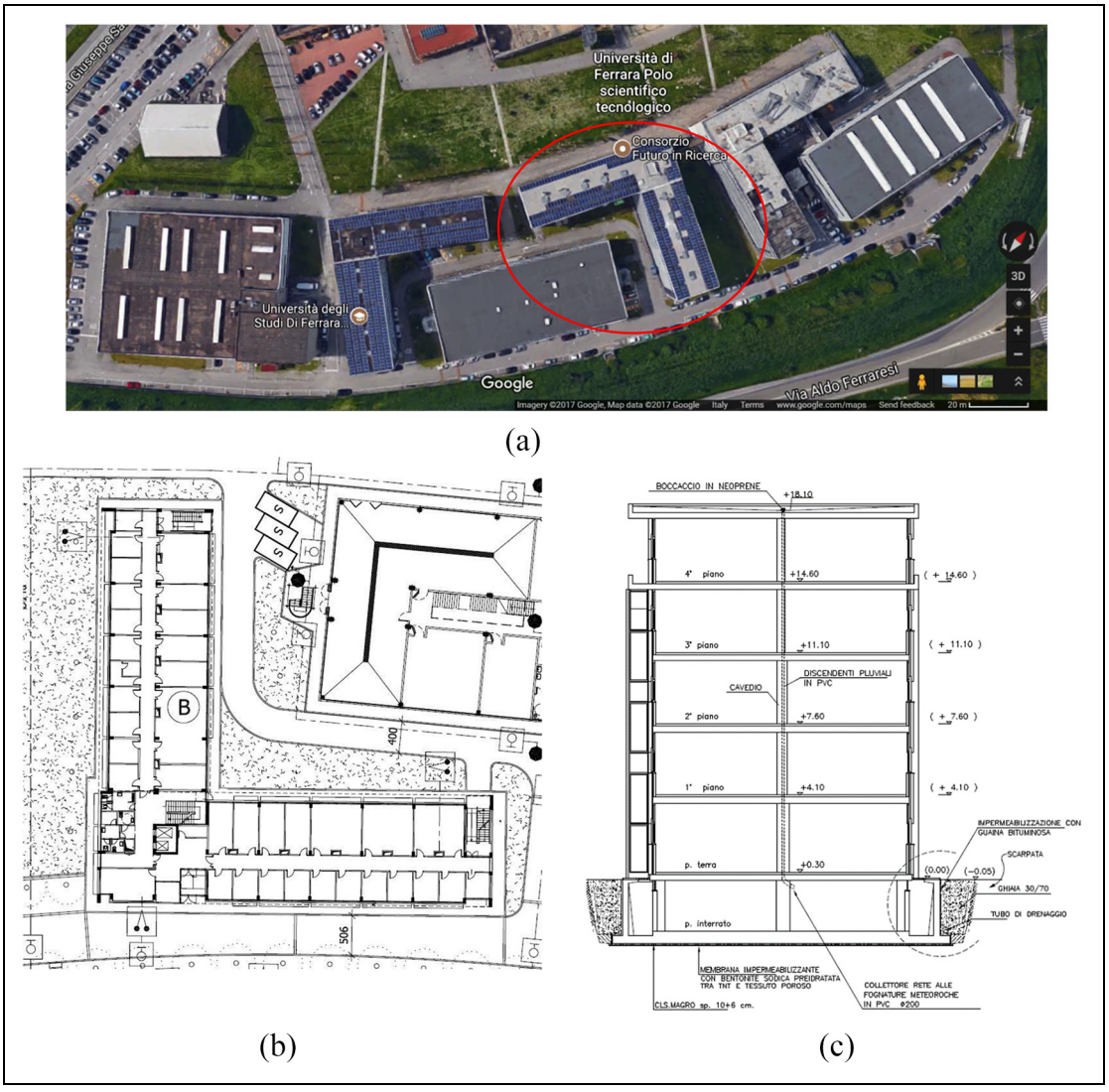

Figure 2. (a) Aerial view of the Technological Scientific Pole. The red circle highlights the investigated building; (b) floor layout and (c) side view of the investigated building.

Building concrete wall septa to keep the center of the forces on the center of the stiffness and prevent the building from rotating;
Rigid anchoring of furniture and lab equipment to the walls;
Reinforcement of the doors of the SDT building first floor (in the NW–SE direction) with metallic supports.

The damage repair intervention was finally completed in September 2012.

SHM

Structural monitoring by means of ambient vibrations represents a very attractive approach because it is low-cost, easy to perform, and non-invasive. Applications include the estimation of frequency trends and related damping (e.g. Ivanović et al.[37] and references therein), evaluation of variations of such quantities as a consequence of earthquakes,[8,21,23,26,38] and finally the calibration of numerical models.[39,40] Ambient vibrations provide a convenient permanent source of shaking, and several methods nowadays leverage on this for the estimation of dynamic properties of buildings. The aspect to keep in mind is that both fundamental vibration frequency and damping significantly depend on the level of shaking. In particular, the building fundamental frequency estimated from the ambient vibration is representative of the building behavior in the linear field, viewed in terms of building–foundation–soil system. It is therefore important to observe this behavior over

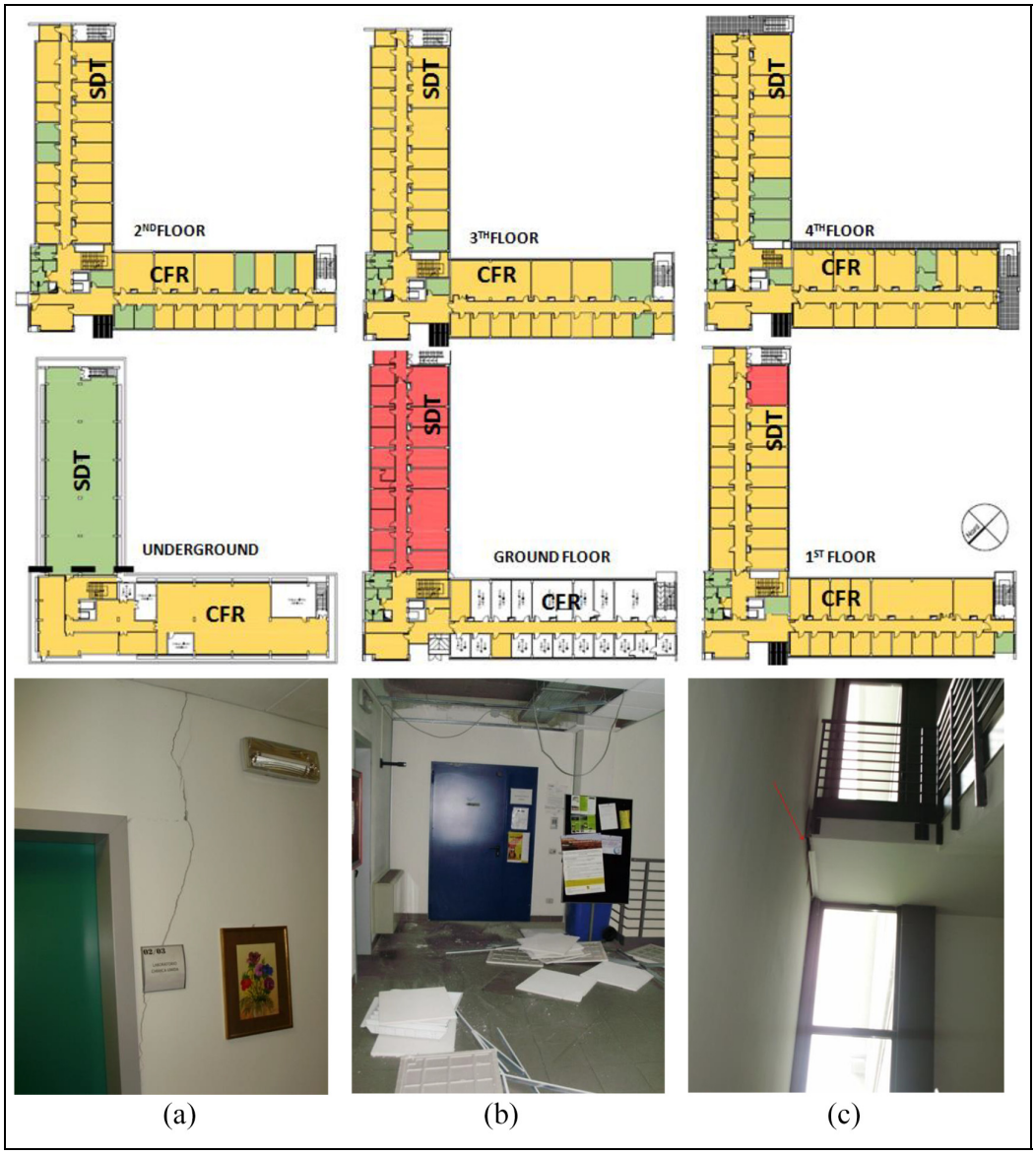

Figure 3. Damage assessment performed at the SDT and CFR blocks of the University of Ferrara (slight damage, in yellow, and medium-severe damage to the infill walls in red): details of the damage (a, c) at the SDT ground floor and (b) at the third floor. The red arrow highlights a gap formed during the earthquake (~3 cm) between the SDT building and the stair body.

their life span, thus accumulating information on their response to different kinds of excitation.

As introduced before, this study evaluated the state of health of the buildings using two different approaches: on-demand AVTs and permanent real-time earthquake (PRT) monitoring. The AVTs were performed at three different times [1] before the earthquake (on 13 April 2012), [2] after the earthquake (on 28 May 2012), and [3] 4 years after repair interventions (on 2 September 2016 and on 11 October 2016). The repair interventions were completed in mid-September 2012. Summarizing, the first AVT [1] (i.e. our fortuitous pre-earthquake measurement) performed at different levels of the buildings was replicated identically during periods [2] and [3]. The tests were conducted in exactly the same locations at each floor (Figure 4). Much of the comparison with the pre-earthquake status is provided through comparisons with the results obtained in [1], while the effect of repairs is better illustrated by comparing [2] and [3]. A preliminary comparison of datasets [1] and [2], performed with a computer code developed at the University of Ferrara, which successively became the core of the OpenHVSR-Processing Toolkit,[41] showed early evidences of the fundamental frequency shift. This, in turn, motivated further studies with more

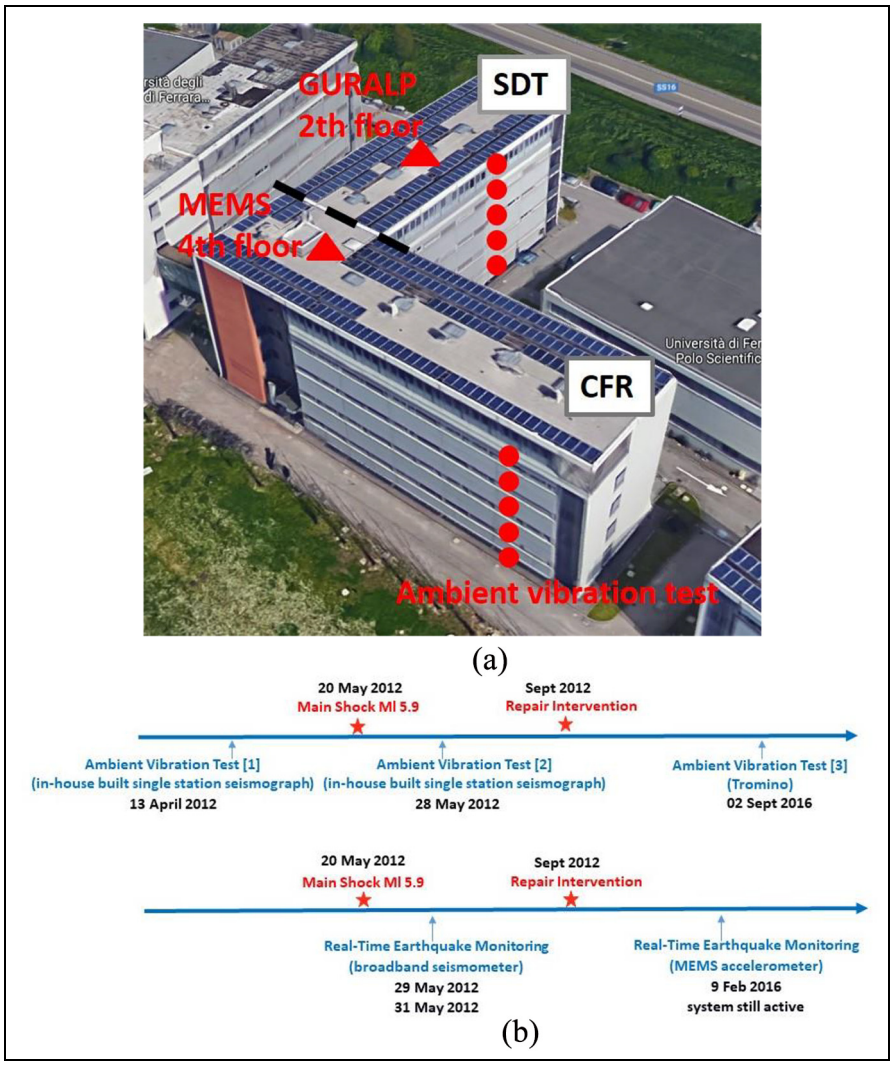

Figure 4. (a) View on the buildings, SDT and CFR sides, seismic joint position (black dashed line), position of the ambient vibration tests, and the real-time monitoring sensors; (b) time evolution of this study.

specific codes (as detailed in the following) and eventually prompted the installation of a permanent monitoring system. Figure 4(a) shows the locations of sensors for both AVTs and earthquake monitoring systems, while in Figure 4(b) we summarize the time evolution of this study.

On-demand AVT

The seismic equipment used for AVT [1] and [2], before and after the mainshock, consisted in an in-house built (Department of Physics and Earth Sciences, University of Ferrara) single-station seismograph based on National Instruments© DAQ-PXI-6120 40 dB gain, 88 V/m/s sensitivity, 18-bit A/D converter connected to a PC. The data logger was connected to a 3C L22 Mark Products seismometer with a natural frequency of 2 Hz. Ambient vibrations were recorded for 40 min at 1000 Hz sampling frequency and then decimated to 125 Hz before processing.

After repairs, AVT [3] was performed using three identical tromographs for seismic ambient microtremor recordings (Tromino, Moho). This instrument features three velocimetric channels (up to ± 1.5 mm/s) working in the frequency range 0.1–1024 Hz, with analog/digital conversion of 24-bit equivalent at 128 Hz. Acquisitions lasted 20 min at 128 Hz sampling frequency. Table 1 summarizes the temporal sequence of measurements, equipment details, the kind of signals acquired, and data analysis.

The ambient vibration recordings were analyzed by HVNSR.[11,26,42,43] The HVNSRs have been estimated by the following procedure: each component is divided into non-overlapping windows of 20 s; each window was detrended, tapered (set to 0.5), padded, fast

Table 1. Details about the on-demand ambient vibration monitoring: period of acquisition, equipment, kind of data acquired, and methods used for the analysis.

Monitoring		Period of acquisition	Equipment	Kind of data	Type of analysis
On-demand	[1]	Before earthquake	In-house developed seismograph (NI electronics)	Ambient vibration	HVNSR NonPaDAn
	[2]	After earthquake	In-house developed seismograph (NI electronics)	Ambient vibration	HVNSR NonPaDAn
	[3]	After repairs	Commercial seismograph model (Tromino, Moho)	Ambient vibration	HVNSR, 3D-XNSR, NonPaDAn

HVNSR: horizontal-to-vertical noise spectral ratio; NonPaDAn: non-parametric damping analysis.

Fourier transformed, and smoothed with triangular windows with a width equal to 5% of the central frequency. For each of the 20-s windows, the arithmetic mean of the two horizontal components' spectra was used to combine E–W and N–S components in the single horizontal (H) spectrum; subsequently, the HVNSR was computed. Finally, the average HVNSR spectrum was obtained, providing also the relative $\pm$ 2 confidence interval. Bonnefoy-Claudet et al.[44] and SESAME Project[45] suggested that strong transients in the signals may affect the estimate, whereas in our experience a simple amplitude variation never caused such a problem.[46,47]

Generally, the HVNSR analysis reveals the fundamental vibration frequency in the two-dimensional (2D) space, that is, on the horizontal plane with a minimum in the vertical direction. This hypothesis might not be verified, especially for buildings that present a strong three-dimensional (3D) directional behavior. To explore this hypothesis, we used the 3D-XNSR (max-to-min spectral ratio) program,[48] which is capable of evaluating along which plane (in space) the fundamental frequency attains its maximum amplitude. In this analysis, the three components of motions are projected on all orthogonal reference systems rotated (in space) with respect to the original one. In this way, the planes for which the spectral ratio is maximum can be individuated. The planes are identified according the azimuth angle (in degrees) with respect to the north and a dip angle (in degrees) with respect to the horizontal plane. The 3D-XNSR analysis produces a diagram in which the x and y coordinates represent the azimuth and dip angles of the investigated plains, respectively. For each couple of such angles, the XNSR analysis is performed and the result is depicted by bullets whose size and color represent the frequency and amplitude of the resulting peak, respectively. This analysis allows us to estimate the building's fundamental frequency for each XY plane in the 3D space.

Finally, the NonPaDAn[14,49] has been applied in order to verify if the damage had also induced a damping variation at the fundamental frequency.

PRT monitoring

Immediately after the mainshock, a 30s–100 Hz broadband CMG-3ESPC Guralp sensor (sensitivity = 1200 V/m/s) connected to a DM24 data logger was installed at the second floor of the SDT building. This sensor monitored the building for 2 days: 29 and 31 May 2012. In February 2016, a Suricat (Moho) micro-electro-mechanical system (MEMS) accelerometer was installed at the fourth floor of the CFR building and the building is still monitored. The Suricat features a set of coupled MEMS accelerometers and achieves the sensitivity and gain of 0.15 mg and 76 μg/count, respectively. Figure 4(a) shows the location of the equipment, while the sensor details are summarized in Table 2.

To discover the intra-event building frequency variation, the earthquake recordings were analyzed using the *S*-transform, which is a time–frequency analysis. In the *S*-transform, a signal is processed using scalable-sliding Gaussian windows, which has the effect of improving the short-time Fourier transform. Subsequently, the continuous wavelet transform is used. The latter operation ensures frequency-dependent resolution while preserving a direct relationship with the Fourier spectrum.[50] With this strategy, building frequency variations, either during or after an earthquake, can be easily observed, hence obtaining an immediate indication of the damage evolution.[3,26]

Results

As a preliminary step, we evaluated the response of the foundation soil in the HVNSR analysis. To do so, we performed two ambient noise acquisitions of 240 min each: one at the basement of the building and the other on the free-field near the foundation. The resulting HVNSR functions, practically identical, highlighted two peaks at low frequencies (0.3 and 0.75 Hz) in agreement with the stratigraphic sequence of the area[30] (Figure 5(a)). Moreover, the spectral stability (Figure 5(b)) shows how these two peaks remain consistently present for the whole duration of the recordings.

Table 2. Sensors used for real-time earthquake monitoring: equipment, period of acquisition, kind of acquired signals, and data analysis.

Monitoring	Sensor	Period of acquisition	Kind of data	Type of analysis
Real-time	CMG-3ESPC (Guralp)	29 May 2012 31 May 2012	Earthquake	S-transform
	Suricat (Moho)	09 February 2016 In acquisition	Earthquake	S-transform

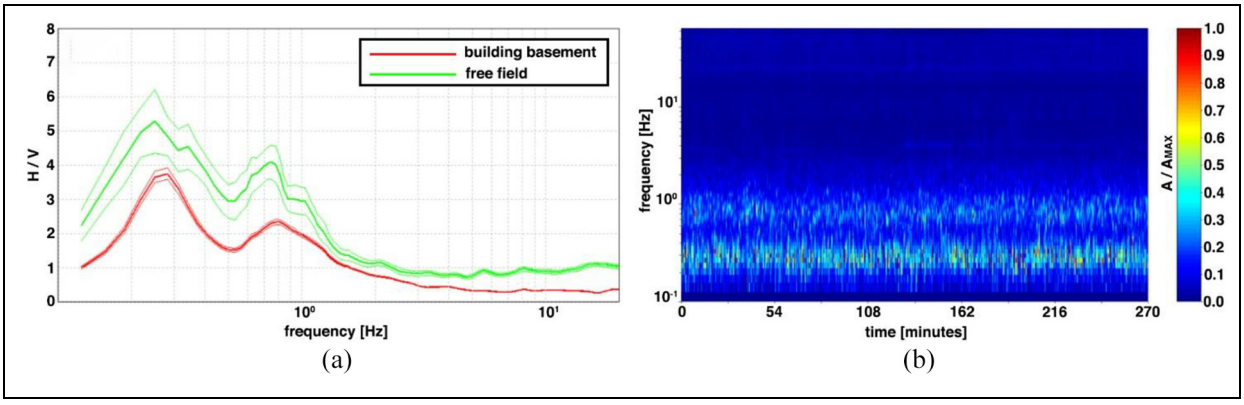

Figure 5. (a) HVNSR curve acquired on the foundation soil and at the building basement; (b) spectral stability (time–frequency analysis).

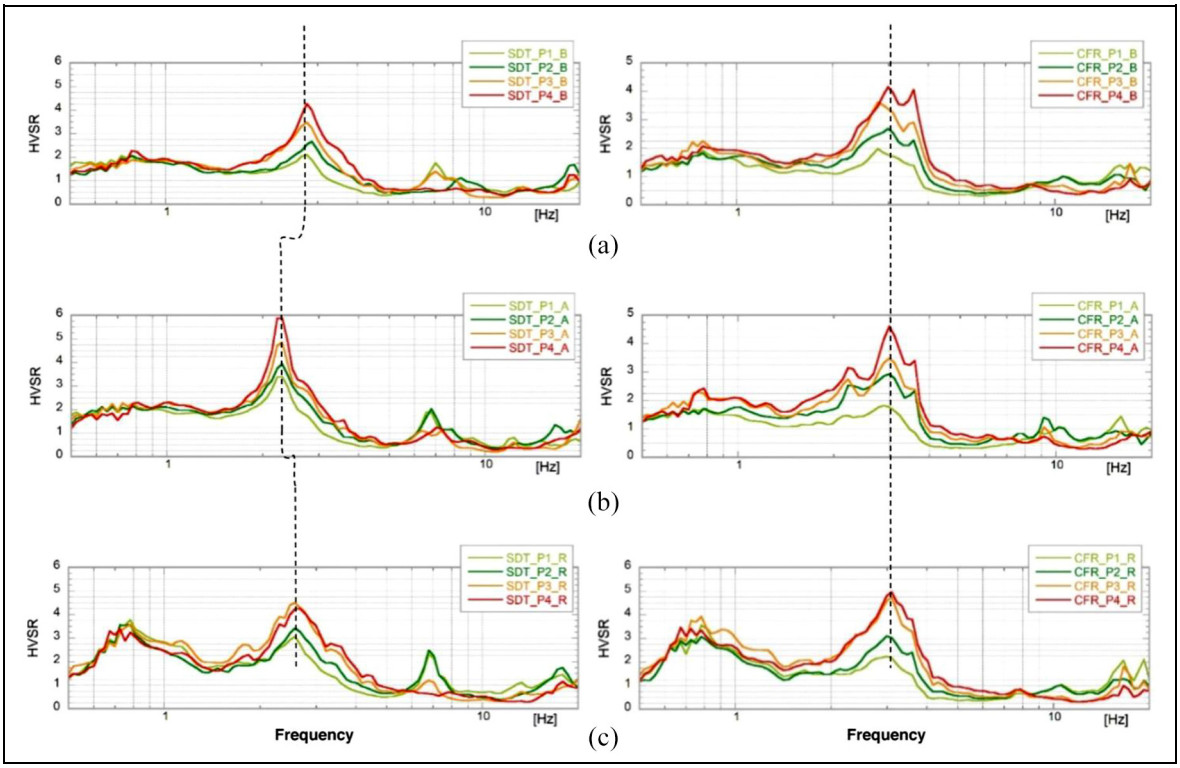

Figure 6. Average HVNSR functions acquired on STD (left) and CFR (right) at each floor. Labels contain the identification of the building, either STD or CFR; the identification of the floor, P1–P4 for the first to the forth level, respectively; and finally, "B,""A," and "R" stand for "before,""after," and "retrofit," respectively. For the sake of clarity, curves are color coded as well: light green for the first floor, green for the second floor, orange for the third floor, and red for the fourth floor. (a) Before the earthquake, (b) after the earthquake, and (c) after damage repair intervention.

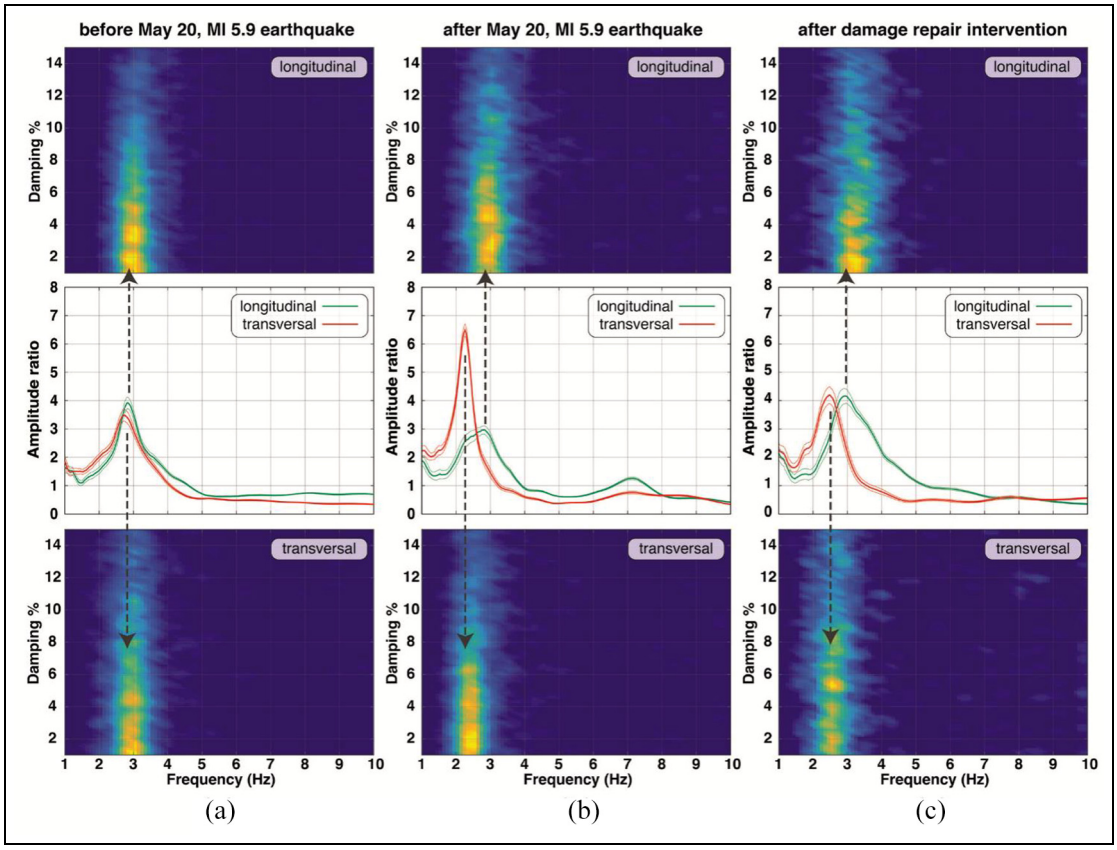

Figure 7. Transversal and longitudinal HVNSR functions acquired on the fourth floor of the STD building (central panel). The damping diagram at the fundamental frequency for the longitudinal (on the top) and transversal (on the bottom) components. Each analysis refers to the data acquired before (a) and after (b) the 20 May M_L = 5.9 earthquake and after the damage repair intervention (c).

Inter-event fundamental frequency and damping variation by ambient vibration tests

All the performed measurements at SDT and CFR buildings were analyzed by the HVNSR technique. Each obtained curve corresponds to the ratio between the arithmetic mean of the two horizontal components' spectra and the vertical spectrum. The curves obtained at each floor are shown in Figure 6. The HVNSRs show a significant and permanent drop of the SDT's fundamental vibration frequency due to the damage. The frequency before the M_L = 5.9 earthquake on 20 May 2012 was 2.9 Hz; during earthquake, it dropped down to 2.2 Hz. Finally, after the damage repair intervention, its original position was nearly restored (approximately 2.7 Hz). Considering the HVNSR functions for each component (longitudinal and transversal directions), it can be noted that the decrease is evident only for the transversal HVNSR function (Figure 7). In fact, the damage was mainly concentrated on the shorter side of the building. The drop of the fundamental frequency is about 24% and, according to the values estimated by Vidal et al.[24] and Ditommaso et al.,[25] it is representative of a slight damage (degree 1 according to the EMS98 scale). Because the damage caused variation of structural stiffness, damping was affected as well. The damping analysis, performed using the NonPaDAn, highlighted a slight change after the earthquake and an even more pronounced variation after the damage repair intervention. The transversal component revealed to be more sensitive to the damping variation. While it was originally in the range of 2%–4%, it slightly increased due to damage. Finally, after the repair intervention, it has become more spread, between 3% and 5% (Figure 7). In contrast, the CFR block did not show any variation of either fundamental frequency or relative damping. The fundamental frequency, at about 3 Hz, remained unchanged both after the earthquake and after the repairs (Figures 6 and 7).

To further our analysis, we investigated the building behavior in the 3D space using the 3D-XNSR approach. Once again, the result, summarized in Figure 8, confirms the observed change of the building fundamental frequency in connection to both damage

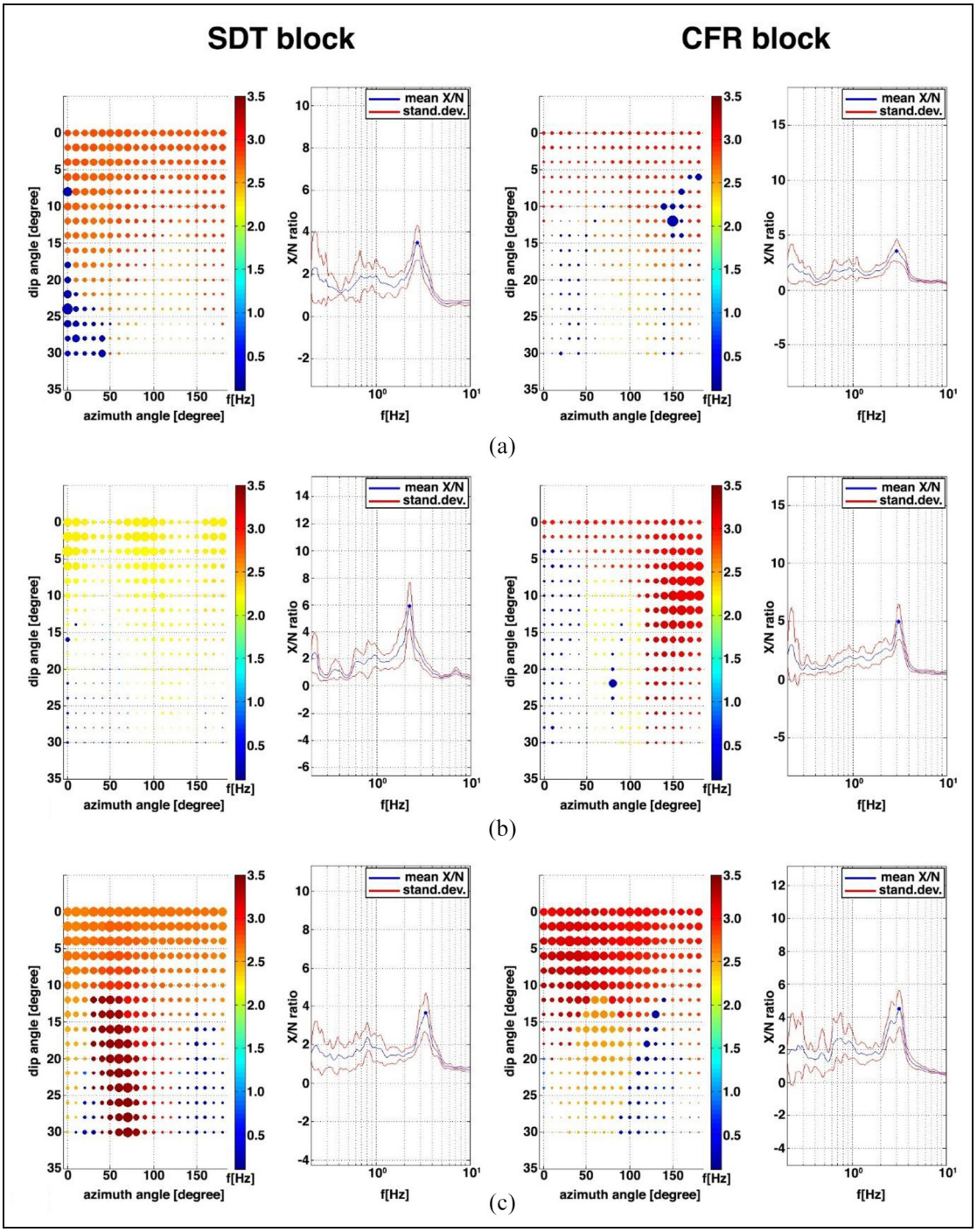

Figure 8. 3D-XNSR directional analysis of ambient vibration recordings for the fourth floor SDT block (left) and for the fourth floor CFR block (right): (a) before the earthquake, (b) after the earthquake, and (c) after seismic retrofitting.

and repairs. Moreover, it provides additional information about the motion of the buildings. On the left side of each panel, the bullet diagrams use coded colors to communicate the fundamental vibration frequency (in hertz). Bullet size stands for peak amplitude, while the x and y coordinates correspond to the azimuth and dip angles describing the building motion. On the right side of each panel, the HVNSR curve is shown as an example for one of the selected bullets. Results for the SDT and CFR buildings are shown, respectively, on both sides. The 3D-XNSR analysis confirmed the clear frequency change initially identified by the HVNSR

analysis for the SDT block. In fact, the color of bullet changes from red (about 3 Hz) to yellow (about 2.2 Hz). In addition, it shows that the building fundamental frequency at 2.9 Hz (before damage) attains its maximum amplification not in the horizontal plane, but on a plane oriented at about 40° with respect to the longitudinal axis and at about 5° with respect to the vertical axis (Figure 8(a), left panel). After damage, the building fundamental frequency settled at about 2.2 Hz and the maximum building motion shifted in a plane oriented at about 90° with respect to the longitudinal axis and at about 5° with respect to the vertical axis (Figure 8(b), left panel). Therefore, the damage not only induced the frequency drop, but also changed the motion plane orientation as well. The repair interventions have further modified the behavior of the building. Two frequencies are evident (Figure 8(c), left panel), one at about 2.7 Hz with the maximum amplitude in the horizontal plane and a second one at about 3.5 Hz with a strong vertical component, probably due to a rocking motion. The damage induced significant variations of the building stiffness, which passed from a "frame with infilled walls" to a "bare frame" behavior. The damage to all infilled walls made the SDT building similar to "bare frame," while the recovery of all infilled walls restored the resistance to lateral forces. From an experimental standpoint, some interesting results regarding the influence of the infill walls on the lateral stiffness and therefore to the fundamental period of vibration were reported by Mucciarelli and Gallipoli[14] and Guler et al.[51] Both studies revealed a frequency increase of about 60% due to the inclusion of infill walls confirming the important contribution of these non-structural components to lateral stiffness.

Unlike the SDT block, in the CFR block, the absence of damage is further confirmed by the absence of frequency drop. The fundamental frequency remains at about 3 Hz as estimated by the HVNSR analysis and NonPaDAn (right panels of Figures 6 and 8), and the building motion remained mainly in the horizontal plane during all the three phases. Nevertheless, the repair intervention introduced a slight vertical component in the building motion. Based on these results, we want to point out that AVTs, performed over time, properly analyzed with the 2D–3D HVNSR and damping analyses, were capable of monitoring the building

Table 3. Earthquakes analyzed in this study.

Date	Time (UTC)	Magnitude	Lat. °N	Lon. °E	Distance (km)	Depth (km)	Sensor	Position
29 May 2012	10:55:56	M_w = 5.3	44.87	10.98	49	4	Guralp	SDT—second floor
29 May 2012	11:00:01	M_L = 5.0	44.86	10.94	52	9	Guralp	SDT—second floor
28 May 2016	03:31:40	M_L = 3.1	44.92	11.29	26	18	Suricat	CFR—fourth floor
26 May 2016	17:10:36	M_w = 5.4	42.88	13.13	249	9	Suricat	CFR—fourth floor

SDT: Scienze della Terra; CFR: Consorzio Futuro in Ricerca.
In light gray are the earthquakes recorded after damage and in dark gray are the earthquakes recorded after the retrofitting intervention. Earthquake information is retrieved from http://cnt.rm.ingv.it.

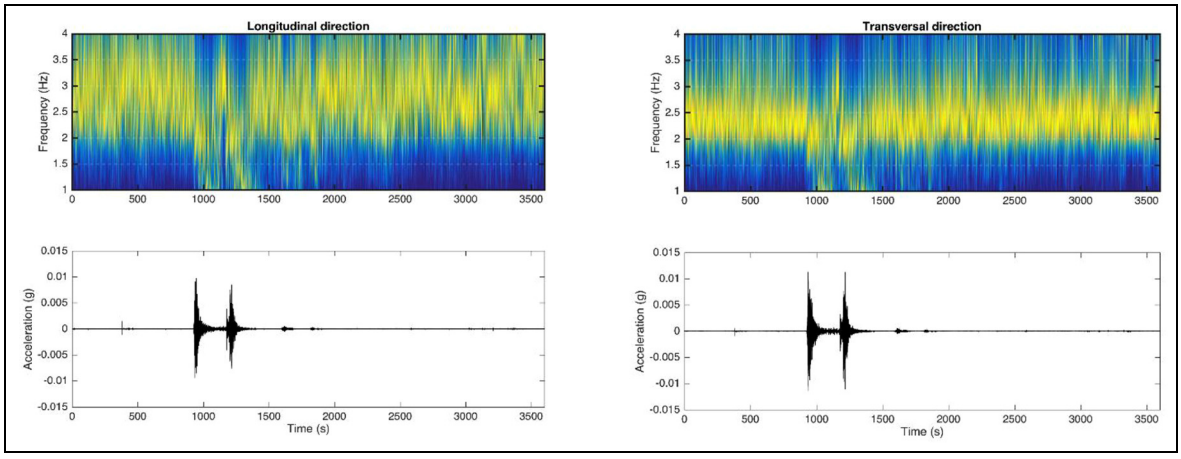

Figure 9. Normalized *S*-transform along the longitudinal (left) and the transversal (right) directions and the corresponding 1-h-long traces comprising both the 29 May 2012, M_w = 5.3 (10:55 UTC) and M_L = 5.0 (11:00 UTC) earthquakes occurred at about 50 km distance from Ferrara.

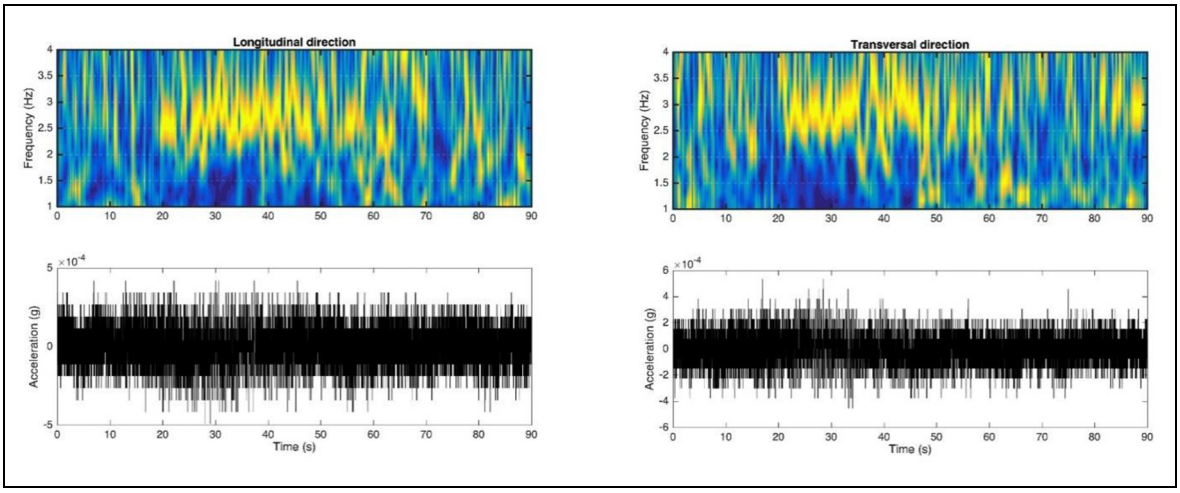

Figure 10. Normalized *S*-transform along the longitudinal (left) and the transversal (right) directions computed using the Suricat accelerogram of a small event of 28 May 2016, M_L = 3.1(03:31 UTC) occurred at about 26 km distance northwest of the building.

health, the evolution of damage, and the effectiveness of repair intervention.

Intra-event fundamental frequency variation by earthquake monitoring

Immediately after the 29 May $M_L = 5.8$ earthquake of the 2012 Emilia seismic sequence, a broadband CMG-3ESPC Guralp sensor connected to a DM24 data logger was placed in the building, at the second floor of the SDT block (Figure 4). On the very same day, the sensor recorded several aftershocks, including the $M_w = 5.3$ (10:55:56 UTC) and $M_L = 5.0$ (11:00:01 UTC) events with epicenters at about 50 km distance from the building (see Table 3). Figure 9 shows the normalized *S*-transform result along the longitudinal (left) and transversal (right) directions for 1-h recording that comprises both the $M \geqslant 5$ aftershocks. The traces were converted to acceleration before the normalized *S*-transform was applied. Results show that the building fundamental frequency temporarily decreased during the two $M \geqslant 5$ events to return to its initial value shortly after. The complete recovery after the two shakes indicates that the building did not suffer further damage. It is noteworthy that the frequencies at about 2.9 and 2.2 Hz along the longitudinal and transversal directions, respectively, are in good agreement with those estimated after damage by the HVNSR and 3D-XNSR techniques (Figure 7(b)).

Real-time damage detection by low-cost MEMS accelerometers

The continuous real-time monitoring of the state of health of this important public building is of course of primary importance in order to ensure that it can be safely used. Mucciarelli et al.[26] demonstrated that the normalized *S*-transform is a suitable tool for the soil and structural dynamic characterization[52,53] even when using seismic ambient noise recordings. As such, in order to implement long-term monitoring of the building, we decided to install the low-cost Suricat system (Moho Srl) and analyze the corresponding data using the *S*-transform, since it guarantees high resolution in both time and frequency domains. The unit, installed at the fourth floor of the CFR (undamaged) building, next to the corner of the L shape (Figure 4), was activated in February 2016 and it is still in acquisition. On 28 May 2016, at 03:31:40 UTC, the Suricat recorded an $M_L = 3.1$ event that occurred at about 26 km distance from Ferrara. Figure 10 shows the normalized *S*-transform of this recording along the longitudinal (left) and transversal (right) directions. Although the shake had small magnitude and the signal-to-noise level was nearly comparable to the electronic noise of the instrument (0.15 mg), the *S*-transform was nevertheless capable of identifying the building's fundamental frequency.

The $M_w = 5.4$ earthquake, on 26 October 2016 (17:10:36 UTC), was also selected for the analyses. This event, which occurred at 249 km distance from the building, belongs to the long-lasting central Italy seismic sequence of 2016–2017. The normalized *S*-transform of this recording is shown in Figure 11, in both horizontal directions (longitudinal and transversal). The fundamental frequency of the building is again retrieved, thus confirming once more the effectiveness of such a low-cost monitoring system. It is worth noting in Figure 11 that, after about 120 s, the accelerogram is dominated by low-frequency coda waves (below 1 Hz), whose frequencies are comparable to the

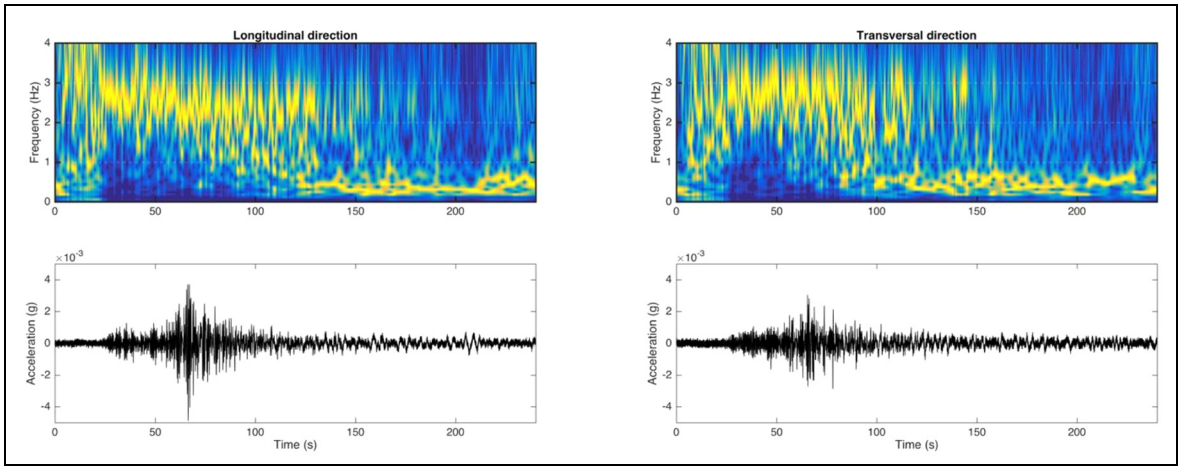

Figure 11. Normalized *S*-transform along the longitudinal (left) and the transversal (right) direction computed using the Suricat accelerogram of the 26 October 2016, M_w = 5.4 central Italy earthquake (17:10:36 UTC) occurred at about 246 km distance south of the building.

natural frequencies of the soil. Both analyses show no frequency variation, meaning that no further damage has occurred.

Discussions and final remarks

The fundamental frequency of two L-shaped, five-story buildings, property of the University of Ferrara (Emilia-Romagna Region, Northern Italy), were estimated before and after the strong seismic event that occurred on 20 May 2012 (the Emilia earthquake) and, finally, after the repair intervention concluded in September 2012. The different monitoring approaches used, on-demand AVTs and permanent earthquake monitoring, and the relevant data analysis provide important insight into the state of health of the buildings, in particular damage identification and evolution, evaluation of structural safety, maintenance quality, and repair effectiveness. The acquired data were investigated using HVNSR, NonPaDAn, 3D-XNSR, and *S*-transform, the first three techniques were capable of estimating the intra-event (before and after the mainshock, and after the repairs) changes of the fundamental vibration frequency and damping, and the *S*-transform analysis captured the inter-event variation of the building fundamental frequency.

It is worth noting that the HVNSR analysis performed on the ambient vibration recordings acquired on 13 April 2012 (i.e. before the 20 May M_L = 5.9 earthquake), both on the free field close to the building and on the building, ensured that the building frequency is distinct enough from the soil's resonance frequency and established a valuable benchmark for subsequent analyses. Subsequently, the comparison between the former dataset (before the earthquake) with analogous results from the HVNSR analysis of ambient vibration recorded after the 20 May M_L = 5.9 earthquake showed a permanent drop of the fundamental frequency from 2.9 to 2.2 Hz. This shift is evident on the transversal component of the recordings acquired on the SDT building whose infill walls suffered slight to moderate damage. The loss of stiffness has caused a decrease in frequency and an increase in damping as well. The 3D-XNSR analysis allowed characterizing the building motion too.

The results obtained by the on-demand AVT suggest that the ambient vibration measurements are suitable for damage detection and may be used for its identification, especially when it is hidden (i.e. there is no visual evidence). As such, this approach represents a very efficient and cost-effective diagnostic method. Moreover, the 3D-XNSR and NonPaDAn applied to ambient vibration data proved to be an efficient analysis technique to evaluate the building state of health and the performance of the repair intervention.

The real-time permanent earthquake monitoring, despite being implemented using low-cost MEMS accelerometers, proved capable of dynamically monitoring the fundamental frequency of the building and track the variation induced by the earthquake, thus constituting a valuable tool for real-time damage detection. In particular, results after the 2-day monitoring with the CMG-3ESPC Guralp sensor confirmed that no further damage was induced on the SDT side of the building by the 29 May M_L = 5.8 earthquake and the two $M \geqslant 5$ aftershocks.

Moreover, the low-cost permanent monitoring systems can be considered a valuable prevention and monitoring tool for judging the state of building health, provided that a pre-disaster building vibrational

behavior is known. As shown, such a reference could be achieved either through continuous monitoring or by ad hoc measurements. Considering that low-cost monitoring systems proved reliable, we suggest that MEMS accelerometers should be extensively installed in seismic-prone urban areas. Such networks would not only monitor the state of health of public and strategic buildings and infrastructure,[3,4,54] but also be suitable to map ground shaking on extended areas for rapid disaster assessment and complete microzonation purposes.[55]

Declaration of conflicting interests

The author(s) declared no potential conflicts of interest with respect to the research, authorship, and/or publication of this article.

Funding

The author(s) disclosed receipt of the following financial support for the research, authorship, and/or publication of this article: This work was funded by project CLARA (Cloud pLAtform and smart underground imaging for natural Risk Assessment, ID code no. SCN_00451).

ORCID iD

Maria Rosaria Gallipoli https://orcid.org/0000-0003-3341-881X

References

1. Stabile TA, Perrone A, Gallipoli MR, et al. Dynamic survey of the Musmeci Bridge by joint application of ground-based microwave radar interferometry and ambient noise standard spectral ratio techniques. *IEEE Geosci Remote Sensing Lett* 2013; 10(4): 870–874.
2. Bursi OS, Zonta D, Debiasi E, et al. Structural health monitoring for seismic protection of structure and infrastructure system. In: Pitilakis K (ed.) *Recent advances in earthquake engineering in Europe, geotechnical, geological and earthquake engineering*, vol. 46. New York: Springer, 2018, pp. 339–358.
3. Gallipoli MR, Stabile TA, Guéguen P, et al. Fundamental period elongation of a RC building during the Pollino seismic swarm sequence. *Case Stud Struct Eng* 2016; 6: 45–52.
4. Mori F and Spina D. Vulnerability assessment of strategic buildings based on ambient vibrations measurements. *Struct Monit Maint* 2015; 2(2): 115–132.
5. Celebi M. *Seismic instrumentation of buildings*. Open-File Report 00-157, 2000, https://pubs.er.usgs.gov/publication/ofr00157
6. Trifunac MD, Ivanovic SS and Todorovska MI. Apparent periods of a buildings: I. Fourier analysis. *J Struct Eng* 2001; 127: 517–526.
7. Trifunac MD, Ivanovic SS and Todorovska MI. Apparent periods of a building: II. Time-frequency analysis. *J Struct Eng* 2001; 127: 527–537.
8. Clinton JF, Bradford SC, Heaton TH, et al. The observed wander of the natural frequencies in a structure. *Bull Seismolsoc Am* 2006; 96: 237–257.
9. Herak M and Herak D. Continuous monitoring of dynamic parameters of the DGFSM building (Zagreb, Croatia). *Bullet Earthquake Eng* 2010; 8(3): 657–669.
10. Castro RR, Mucciarelli M, Pacor F, et al. Determination of the characteristic frequency of two dams located in the region of Calabria, Italy. *Bull Seism Soc Am* 1998; 88(2): 503–511.
11. Gallipoli MR, Mucciarelli M, Castro RR, et al. Structure, soil–structure response and effects of damage based on observations of horizontal-to-vertical spectral ratios of microtremors. *Soil Dyn Earthquake Eng* 2004; 24: 487–495.
12. DiGiulio G, Azzara RM, Cultrera G, et al. Effect of local geology on ground motion in the city of Palermo, Italy, as inferred from aftershocks of the 6 September 2002Mw 5.9 earthquake. *Bull Seismol Soc Am* 2005; 95: 2328–2341.
13. Parolai S, Facke A, Richwalski SM, et al. Assessing the vibrational frequencies of the Holweide Hospital in the city of Cologne (Germany) by means of ambient seismic noise analysis and FE modelling. *Nat Hazards* 2005; 34: 217–230.
14. Mucciarelli M and Gallipoli MR. Damping estimate for simple buildings through non-parametric analysis of a single ambient vibration recording. *Ann Geophys* 2007; 50: 259–266.
15. Cole MA. *On-line failure detection and damping measurements of aerospace structures by random decrement signature*. NASA CR-2205, 1973, https://ntrs.nasa.gov/archive/nasa/casi.ntrs.nasa.gov/19730010202.pdf
16. Clough RW and Penzien J. *Dynamics of structures*. 2nd ed. New York: McGraw-Hill, 1975.
17. Trifunac MD. Comparisons between ambient and forced vibration experiments. *Earthquake Eng Struct Dyn* 1972; 1(2): 133–150.
18. Gallipoli MR, Mucciarelli M and Vona M. Empirical estimate of fundamental frequencies and damping for Italian buildings. *Earthquake Eng Struct Dyn* 2009; 38(8): 973–988.
19. Dunand F. *Pertinence du bruit de fond sismique pour la caracte'risation dynamique et l'aide au diagnostic sismique des structures de ge'nie civil*. PhD Thesis, Université Joseph-Fourier-Grenoble I, Grenoble, 2005.
20. Mikael A, Gueguen P, Bard P-Y, et al. The analysis of long-term frequency and damping wandering in buildings using the random decrement technique. *Bull Seismol Soc Am* 2013; 103(1): 236–246.
21. Mucciarelli M, Gallipoli MR, Masi A, et al. Analysis of RC building dynamic response and soil-building resonance based on data recorded during a damaging earthquake (Molise, Italy 2002). *Bull Seismol Soc Am* 2004; 94(5): 1943–1953.
22. Michel C, Guéguen P, El Arem S, et al. Full-scale dynamic response of an RC building under weak seismic motions using earthquake recordings, ambient vibrations and modelling. *Earthquake Eng Struct Dyn* 2010; 39(4): 419–441.

23. Calvi GM, Pinho R and Crowley H. State-of-the-knowledge on the period elongation of RC buildings during strong ground shaking. In: *Proceedings of the first European conference on earthquake engineering and seismology*, Geneva, 3–8 September 2006, p. 1535, http://citeseerx.ist.psu.edu/viewdoc/download?doi = 10.1.1.588.7836&rep = rep1&type = pdf
24. Vidal F, Navarro M, Aranda C, et al. Changes in dynamic characteristics of Lorca RC buildings from pre- and post-earthquake ambient vibration data. *Bull Earthquake Eng* 2013; 12(5): 2095–2110.
25. Ditommaso R, Vona M, Gallipoli MR, et al. Evaluation and considerations about fundamental periods of damaged reinforced concrete buildings. *Natural Haz Earth Syst Sci* 2013; 13(7): 1903–1912.
26. Mucciarelli M, Bianca M, Ditommaso R, et al. Far field damage on RC buildings: the case study of the Navelli during the L'Aquila (Italy) seismic sequence 2009. *Bull Earthquake Eng* 2011; 9: 263–283.
27. Masi A, Santarsiero G, Gallipoli MR, et al. Performance of the health facilities during the 2012 Emilia (Italy) earthquake and analysis of the Mirandola hospital case study. *Bull Earthquake Eng* 2014; 12(5): 2419–2443.
28. Michel C, Guéguen P and Bard PY. Time-frequency analysis of small frequency variations in civil engineering structures under weak and strong motions using a reassignment method. *Struct Health Monit* 2010; 9(2): 159–171.
29. Galli P, Castenetto S and Peronace E. The MCS macroseismic survey of the Emilia 2012 earthquakes. *Ann Geophys* 2012; 55(4): 663–672.
30. Priolo E, Romanelli M, Barnaba C, et al. The Ferrara thrust earthquakes of May-June 2012: preliminary site response analysis at the sites of the OGS temporary network. *Ann Geophys* 2012; 55(4): 591–597.
31. Tertulliani A, Arcoraci L, Berardi M, et al. The Emilia 2012 sequence: a microseismic survey. *Ann Geophys* 2012; 55(4): 679–687.
32. Govoni A, Marchetti A, De Gori P, et al. The 2012 Emilia seismic sequence (Northern Italy): imaging the thrust fault system by accurate aftershock location. *Tectonophysics* 2014; 622: 44–55.
33. Magliulo G, Ercolino M, Petrone C, et al. The Emilia earthquake: seismic performance of precast reinforced concrete buildings. *Earthquake Spectra* 2014; 30(2): 891–912.
34. Baggio C, Bernardini A, Colozza R, et al. *Manuale per la compilazione della scheda di 1° livello di rilevamento danno, pronto intervento e agibilità per edifici ordinari nell'emergenza post-sismica (AeDES)*. ©PCM-DPC (in Italian), 2014, http://www.protezionecivile.gov.it/media-comunicazione/pubblicazioni/dettaglio/-/asset_publisher/default/content/manuale-per-la-compilazione-della-scheda-di-1-livello-di-rilevamento-di-danno-pronto-intervento-e-agibilita-per-edifici-ordinari-nell-emergenza-post-s
35. Masi A, Santarsiero G, Digrisolo A, et al. Procedures and experiences in the post-earthquake usability evaluation of ordinary buildings. *Bollet Geofis Teor Appl* 2016; 57(2): 199–220.
36. Grünthal G (ed.). European Macroseismic Scale 1998 (EMS-98), European Seismological Commission, sub commission on Engineering Seismology, Working Group Macroseismic Scales, 1998, http://www.franceseisme.fr/EMS98_Original_english.pdf
37. Ivanović SS, Trifunac MD, Novikova EI, et al. Ambient vibration tests of a seven-story reinforced concrete building in Van Nuys, California, damaged by the 1994 Northridge earthquake. *Soil Dyn Earthquake Eng* 2000; 19(6): 391–411.
38. Régnier J, Michel C, Bertrand E, et al. Contribution of ambient vibration recordings (free-field and buildings) for post-seismic analysis: the case of the Mw 7.3 Martinique (French lesser Antilles) earthquake, November 29, 2007. *Soil Dyn Earthquake Eng* 2013; 50: 162–167.
39. Celebi M. Before and after retrofit—response of a building during ambient and strong motions. *J Wind Eng Ind Aero Dyn* 1998; 77–78: 25968.
40. Ventura C, Liam Finn W-D, Lord JF, et al. Dynamic characteristics of a base isolated building from ambient vibration measurement and low level earthquake shaking. *Soil Dyn Earthquake Eng* 2003; 23: 313–322.
41. Bignardi S, Yezzi AJ, Fiussello S, et al. OpenHVSR—processing toolkit: enhanced HVSR processing of distributed microtremor measurements and spatial variation of their informative content. *Comput Geosci* 2018; 120: 10–20.
42. Mucciarelli M. Reliability and applicability of Nakamura's technique using microtremors: an experimental approach. *J Earthquake Eng* 1998; 2(4): 625–638.
43. Chavez-Garcia FJ and Cardenas-Soto M. The contribution of the built environment to the "free-field" ground motion in Mexico City. *Soil Dyn Earthquake Eng* 2002; 22: 773–780.
44. Bonnefoy-Claudet S, Cornou C, Bard P-Y, et al. H/V ratios: a tool for site effects evaluation. Results from 1-D noise simulations. *Geophys J Int* 2006; 167: 827–837.
45. SESAME Project. *Guidelines for the implementation of the H/V spectral ratio technique on ambient vibrations. Measurements, processing and interpretation*. WP12, Deliverable N. D23.12, 2004, ftp://ftp.geo.uib.no/pub/seismo/SOFTWARE/SESAME/USER-GUIDELINES/SESAME-HV-User-Guidelines.pdf
46. Parolai S and Galiana-Merino JJ. Effect of transient seismic noise on estimates of H/V spectral ratios. *Bull Seismol Soc Am* 2006; 96: 228–236.
47. Mucciarelli M. Jumpin' joy quake. *Seismol Res Lett* 2007; 77: 744–745.
48. Mucciarelli M, Stabile TA, Gallipoli MR, et al. XNSR—a software for a different approach to single-station spectral ratio In: *Proceedings of the ESC-2016 35th general assembly, Session 1*, Trieste, 4–10 September 2016.
49. Gallipoli MR, Mucciarelli M, Šket-Motnikar B, et al. Empirical estimates of dynamic parameters on a large set of European buildings. *Bull Earthquake Eng* 2010; 8: 593–607.
50. Stockwell RG, Mansinha L and Lowe RP. Localization of the complex spectrum: the S transform. *IEEE Trans Sig Proc* 1996; 44: 998–1001.

51. Guler K, Yuksel E and Kocak A. Estimation of the fundamental vibration period of existing RC buildings in Turkey utilizing ambient vibration records. *J Earthquake Eng* 2008; 12(Suppl. 2): 140–150.
52. Parolai S. Denoising of seismograms using the S transform. *Bull Seismol Soc Am* 2009; 99(1): 226–234.
53. Ditommaso R, Mucciarelli M and Ponzo FC. S-Transform based filter applied to the analysis of nonlinear dynamic behaviour of soil and buildings. In: *Proceedings of the 14th European conference on earthquake engineering*, Ohrid, Republic of Macedonia, 30 August–3 September 2010.
54. Bindi D, Petrovic B, Karapetrou S, et al. Seismic response of an 8-story RC-building from ambient vibration analysis. *Bull Earthquake Eng* 2015; 13: 2095–2120.
55. D'Alessandro A, Luzio D and D'Anna G. Urban MEMS based seismic network for post-earthquakes rapid disaster assessment. *Adv Geosci* 2014; 40: 1–9.